Transactions of the SMiRT 27
Yokohama, Japan, March 3-8, 2024
Division V

EVALUATION OF THE APPLICABILITY OF SEISMIC PERFORMANCE VERIFICATION INDICES FOR RELATIVE DISPLACEMENT IN REINFORCED CONCRETE MEMBERS

Satoshi Komatsu[1], Yoshinori Miyakawa[2] and Toyofumi Matsuo[3]

[1] Associate Professor, Yokohama National University, Kanagawa, Japan (komatsu-satoshi-yx@ynu.ac.jp)
[2] Senior research scientist, Central Research Institute of Electric Power Industry, Japan
[3] R&D Manager, Central Research Institute of Electric Power Industry, Chiba, Japan

ABSTRACT

In this paper, we deal with refining and standardizing seismic performance verification methods for reinforced concrete (RC) underground structures (box culverts) serving as emergency cooling facilities in nuclear power plants. In our previous research, the applicability of two deformation indices related to displacement of concrete members was verified for full-scale RC columns experiencing shear or bending failure under bilateral loads. The indices were “Thickness increment of RC member” assuming out-of-plane shear failure and “Relative displacement on compressive edge in RC member” assuming in-plane shear failure and out-of-plane bending failure. However, verification could not be performed satisfactorily under the conditions of the environment in which the structure was in use. Therefore, in this study, the applicability of these indices is investigated for full-scale RC columns with varying axial force ratios or member shapes (aspect ratios).

INTRODUCTION

Verification methods involving numerical analysis are becoming widely used for determining the seismic safety of concrete structures. Non-linear time-dependent analysis considering the integrated mechanical behavior of the ground and structures has become the standard evaluation method (Nuclear Civil Engineering Committee 2021) for investigating reinforced concrete (RC) underground structures that constitute the emergency cooling facility of a nuclear power plant, as depicted in Figure 1.

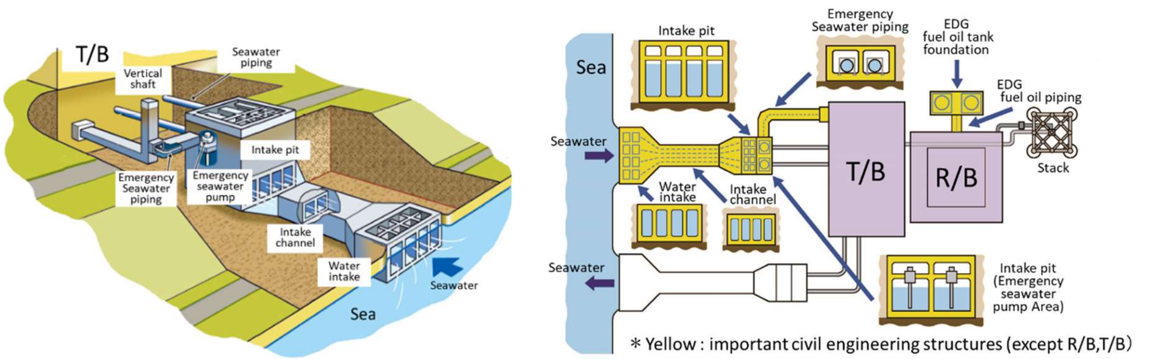

Figure 1. Underground structures in a nuclear power station.

A unique feature of these structures is that they are unoccupied when the power plants are in operation. Thus, the seismic performance requirement is that box culverts should withstand standard seismic motion so as to maintain the functionality of equipment and piping and to ensure water flow during emergencies (Nuclear Civil Engineering Committee 2021). Therefore, developing a method to judiciously verify the load-carrying capacity of these structures is necessary. The reason for this is that existing verification indices are often designed with excessive safety features for reasons such as insufficient consideration of structural redundancy (JSCE 2018; Komatsu et al. 2021).

Based on this background, an index called "Thickness increment of RC member" has been proposed and verified (Miyagawa et al. 2018). The index considers the relationship between diagonal tensile failure and crack width in the RC member, enabling the rational evaluation of the load-carrying capacity of RC members with out-of-plane shear failure. Another index, "Relative displacement on compressive edge in RC member", has been proposed to evaluate failure modes induced by compressive failure of concrete, such as in-plane shear failure and out-of-plane bending failure (Komatsu et al. 2023).

In previous research, the applicability of the two proposed deformation indices related to the displacement of concrete members has been verified for full-scale RC members with shear or bending failure under bilateral loads (Komatsu et al. 2023). In summary, numerical studies have focused on the development of advanced verification indices or limiting values for performance verification through nonlinear material analysis, as indicated by the data in Table 1 (Nuclear Civil Engineering Committee 2021). It was found that these indices are insensitive to local damage and meshing element geometry, enhancing the precision of performance verification.

Table 1: Verification indices for failure modes.

Failure pattern	Direction	Failure mode	Verification index
Shear	Out-of-plane	Diagonal tension failure	Thickness increment of RC member
		Shear compression failure	Relative displacement on compressive edge in RC member
	In-plane		
Flexure	Out-of-plane	Flexural compression failure	

However, it was not possible to adequately verify the indices under conditions that simulate the environment in which the structures would be used. Therefore, in this study, the applicability of these indices was investigated for full-scale RC columns with different axial force ratios or member shapes (aspect ratios).

DEFINITION OF THE INDICES

Each of the indices proposed by the authors and their limit values are summarized here. For a comprehensive understanding of the derivation and limit values of these indices, the reader is referred to relevant published papers and guidelines (Komatsu et al. 2023; Nuclear Civil Engineering Committee 2021).

Thickness Increment of RC Member

"Thickness increment of RC member", which indicates the degree of expansion in the thickness of the member, as indicated in Eq. (1), is mainly due to diagonal cracks (X-shaped cracks) and bond splitting cracks and roughly corresponds to the total of these openings. This can be applied to both one-way and repetitive loadings.

$$\Delta D_{lim} = max\{5,\ 2.5 p_w D\} \tag{1}$$

where ΔD_{lim} is the limit value of thickness increment of the RC member (in mm), p_w is the shear reinforcement ratio, and D is the member thickness (mm).

The left panel in Figure 2 depicts the node configuration used in the calculation. This index is effective as an evaluation index for assessing out-of-plane shear failure because it does not detect the opening of bending cracks but does detect the opening of diagonal shear cracks.

In this study, the relative displacement between element nodes at the same elevation was calculated, and the maximum value was adopted.

The first term (5 mm) focuses on members lacking out-of-plane shear reinforcing bars. According to previous experiments with member thicknesses ranging from 400 mm to 800 mm and axial force ratios from -0.05 to 0.05, the residual rate of load-carrying capacity in the direction perpendicular to the member axis is between 60% and 95% when the thickness expands by 5 mm (Miyagawa et al. 2014). The second term ($2.5p_wD$) considers the distribution of cracks due to the use of shear reinforcing bars. Analytical case studies have revealed the relationship expressed in Eq. (2) in members with different specimen lengths, reinforcing bar ratios, and reinforcing bar diameters.

$$\varepsilon_{ave} = 2.5p \qquad (2)$$

where ε_{ave} is the average strain and p is the shear reinforcing bar ratio (direct value, not expressed in %). The displacement index is obtained by multiplying the average strain ε_{ave} by the member thickness D.

For this index, the limit state is defined as the situation where the horizontal load-carrying capacity of a statically indeterminate structure is retained, even if the carrying capacity of members is slightly reduced. In other words, this index is not assumed to be applied to statically indeterminate structures because a decrease in the load-carrying capacity of members directly leads to a decrease in the horizontal load-carrying capacity of the structure.

Relative Displacement on Compressive Edge in RC Member

The "Relative displacement on compressive edge in RC member" is 2 mm, indicating the relative displacement between nodes 200 mm away from the member edge at the compressive edge of the RC member, as given in Eq. (3). The node image used for the calculation is shown in Fig. 2 (right panel).

$$\Delta l_{lim}' = 2.0 \qquad (3)$$

where $\Delta l_{lim}'$ is the limit value of relative displacement on the compressive edge (mm). However, the node used for verification must be at least 200 mm away from the end of the member, excluding the haunch.

This index is based on the same idea (limit state, applicable structure type) as the "Thickness increment of RC member." Therefore, the applicable conditions are the same as "Thickness increment of RC member" .

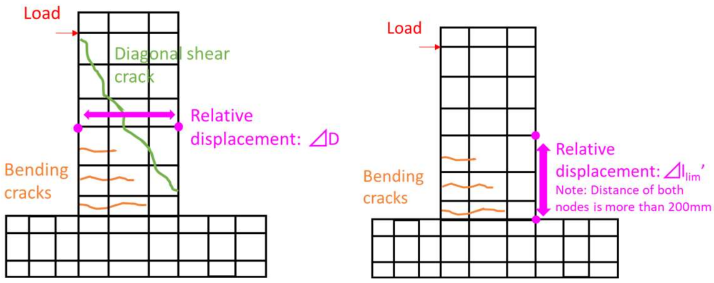

Figure 2. Image of the proposed seismic performance verification index in the RC member. (Left, Thickness increment of RC member; Right, Relative displacement on compressive edge in RC member).

OUTLINE OF EXPERIMENTS

Specimen Outline

Figure 3 shows the dimensions of each specimen, designed in accordance with the structural specifications (dimensions and bar arrangement status) of actual-scale members in the structure. The specimens were configured as columns with footing. The bar arrangement conditions in cases N-1, N-2-1, and N-2-2 were all designed to cause shear failure. The distinction between these cases lies in the loading process, as explained in a later section. Assuming seismic retrofitting, a specimen (P-1) with post-installed shear reinforcing bars was prepared. These bars in specimen P-1 were placed on one side, considering on-site construction conditions, such as retrofitting side walls of underground culverts, which involve backfill and for which any construction activity can be executed only from inside of the culverts.

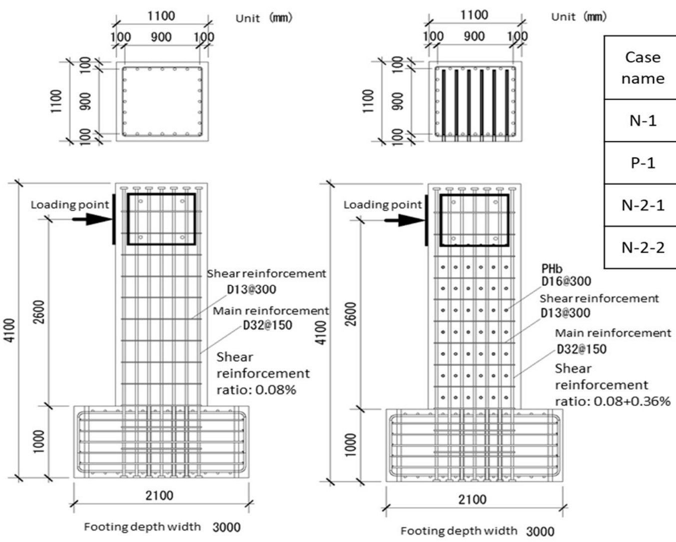

Case name	Shear reinforcement ratio(%)	Loading pattern	Fracture behavior	Loading age[days]
N-1	0.08	1	Diagonal shear failure	82
P-1	0.08+0.36 (post installed)	1	Compressive bending failure	90
N-2-1	0.08	2	Diagonal shear failure	97
N-2-2	0.08	3	Compressive shear failure	104

Figure 3. Overview of the specimens. (Left, N-1, N-2-1, N-2-2; Right, P-1).

Material Properties

Table 2 shows the physical characteristics of concrete and reinforcing bars. The tensile strength was calculated by conversion from the compressive strength (JSCE 2018). The compressive strength and Young's modulus were measured on the loading date.

Table 2: Material properties of the concrete and reinforcing bars.

Case Name	Compressive strength [N/mm^2]	Young's modulus [kN/mm^2]	Tensile strength [N/mm^2]
N-1	36.9	30.0	2.5
P-1	36.2	29.9	2.5
N-2-1	39.1	30.8	2.6
N-2-2	39.0	30.7	2.6

	Yielding strength [N/mm^2]	Tensile strength [N/mm^2]	Young's modulus [kN/mm^2]
Main rebar (D32)	508	676	196
Shear rebar (D13)	360	476	188
Post-installed shear rebar (D16)	396	584	188

State of Loading Patterns

The loading patterns are depicted in Figure 4. The square shape "□" in the figure represents the column viewed from directly above, with loading direction 1 from bottom to top and loading direction 2 from left to right. No axial forces acted on the columns during the experiment.

In the cases of N-1 and P-1, the specimens were loaded monotonically until the maximum load was reached. Case N-2-1 followed the same procedure as N-1 and P-1, but with the loading direction rotated by 45 degrees. In the case of N-2-2, positive and negative alternating loading was first applied until diagonal cracks occurred; after that, the loading direction was rotated by 90 degrees, and the specimen was loaded monotonically until the maximum load was reached.

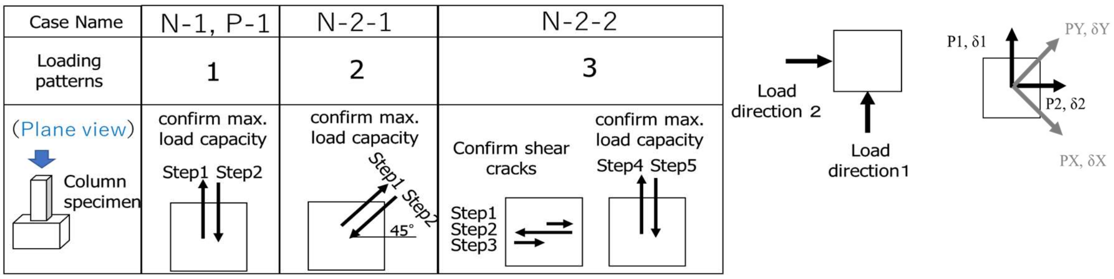

Figure 4. Loading pattern for each specimen.

Summary of Experimental Results

Figure 5 shows the load-displacement relationship for each specimen. The failure modes were diagonal tensile failure for N-1 and N-2-1, flexural failure for P-1, and compressive shear failure for N-2-2. Notably, N-2-2 represents loading step 4, which is loading after pre-crack (loading steps 1 to 3).

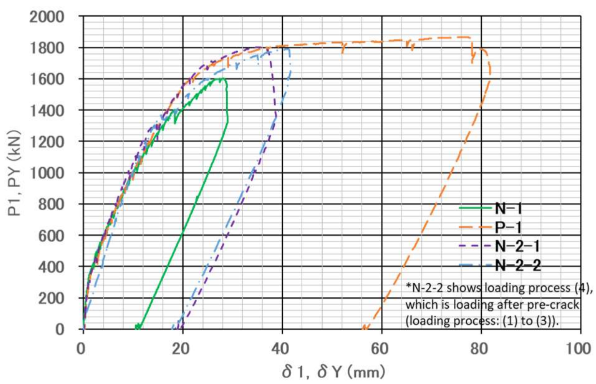

Figure 5. Load-displacement relationship in different RC members.

OUTLINE OF ANALYSIS

Analysis Method

In this study, we used a three-dimensional material nonlinear finite element method analysis program (COM3). This program is a three-dimensional extension of the RC plane model based on a material nonlinear configuration model that considers any loading history and which has demonstrated high analysis accuracy (Maekawa et al. 2003). To extend the 2D RC plane model to 3D, the main axis is set perpendicular to the first crack plane, and the second and third axes are set orthogonal to the first crack plane. The two-dimensional RC constitutive law is applied to these three axial planes, and the three-dimensional stress state is expressed by superimposing stress transmissions. The RC plane model defines the average stress-strain relationship by averaging the behavior of multiple fine cracks in a finite volume (smeared crack model). The average stress-strain relationship of concrete consists of one-dimensional compression, tension, and shear transfer models of cracked surfaces. By using the multi-directional non-orthogonal fixed crack model, it is possible to reproduce the occurrence and post-occurrence of multi-directional cracks occurring in response to the loading history.

Mesh Divisions

Figure 6 shows the mesh used to represent the specimens in this study. In order to satisfactorily consider the effect of bonding between the reinforcing bar and concrete regardless of the element size, the main reinforcing bar was placed at the center of the RC element cross section (Maekawa et al. 2003). A plane concrete element was placed in the area into which the bonding does not extend. In the modeling, the number of post-installed shear reinforcing bars was sufficiently large so that they could be treated as uniformly dispersed in the core concrete at a constant reinforcing bar ratio.

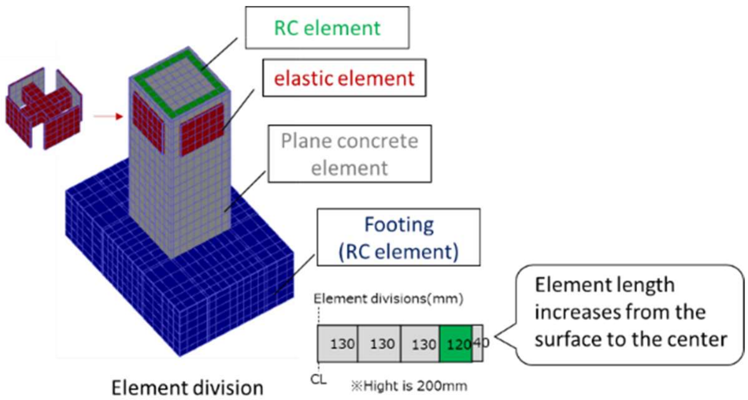

Figure 6. Mesh representing the specimens.

Material Properties

Basically, material mechanical properties performed in accordance with JIS (Japanese Industrial Standards) tests were set as input values. . Regarding the tensile strength of concrete, it has been reported that the accuracy of this property can be improved by reducing the apparent tensile strength because of the shrinkage stress generated on the concrete surface due to volume change due to hydration hea, autogenous shrinkage and drying shrinkage (Nuclear Civil Engineering Committee 2021). In this study, the tensile strength was reduced to 60%.

To account for the bonding effect between the reinforcing bar and concrete after crack initiation, the following equation has been proposed.

$$\sigma_t = f_t(\varepsilon_{tu}/\varepsilon_t)^c \qquad (4)$$

where σ_t is the tensile stress of concrete (N/mm^2), f_t is the uniaxial compressive strength of concrete (N/mm^2), ε_{tu} is the strain at crack initiation, ε_t is the average tensile strain of concrete, and c is the tensile stiffening coefficient. The tensile stiffening coefficients in RC elements were 0.4 in the main reinforcing bar axial direction, 0.8 in the shear reinforcing bar direction, and 2.0 in the reinforcing bar orthogonal direction. The tensile softening coefficient in plane concrete elements was determined according to the element dimensions (Maekawa et al. 2003).

Axial Force and Aspect Ratio (Member Size)

When evaluating the influence of the axial force ratio, the analytical condition is set to the condition (0.3), which is considered to be the maximum for an underground RC box culvert. The size of the columns is the same as that under the experimental conditions (Komatsu et al. 2023).

The model is then extended to the upper and lower limits of the member thickness of the actual structure (440 mm and 4,400 mm) to assess the effect of the column shape (aspect ratio) as shown in Table 2. In the actual reinforcement arrangement of the structure, the concrete cover is uniform at 100 mm, regardless of the member thickness, and the middle reinforcing bars are placed at equal intervals. The reinforcement ratio is modeled to be the same regardless of member thickness. Different sizes of loading plates are set for each model so that the load is applied to the entire surface. The influence of axial forces is not considered here. An overview of the specimen is shown in Figure 7.

Table 3: List of cases to be considered for numerical simulation.

Axial force ratio	Aspect ratio (size of the member)		
	7.0 (440×440 mm)	2.8 (1100×1100 mm)	0.7 (4400×4400 mm)
0	X	X*	X
0.3		X	

*Experimental condition

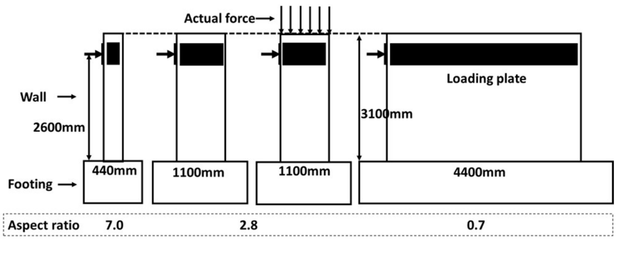

Figure 7. overview of the specimens in numerical simulation.

RESULTS OF THE ANALYSIS

The validation results of the applicability of the analytical model compared with the experimental results are presented in a published paper (Komatsu et al. 2023). The results of the numerical experiments conducted by applying the analytical model are discussed below.

Verification of the Influence of Axial Force Ratio (0 or 0.3)

The applicability of both indices is assessed under the condition that a predetermined axial force is applied in the vertical downward direction (gravitational direction) from the column top to the model. Each analysis case is identified using the axial force ratio indicated at the end of the loading pattern in Figure 4 (e.g., "N-1_ax0.3"). The load-displacement relationship (red line) in each case and the points where both indices reached the limit values are indicated by the symbol "○" on the load-displacement relationship in Figure 8. "Thickness increment of RC member" ΔD_{lim} is marked as a positive value, and "Relative displacement on compressive edge in RC member" $\Delta l_{lim}{}'$ is marked as a negative value on the graph.

In N-2-1_ax0.3 and N-2-2_ax0.3, the index that reaches the limit value is replaced with that when the axial force ratio is 0.

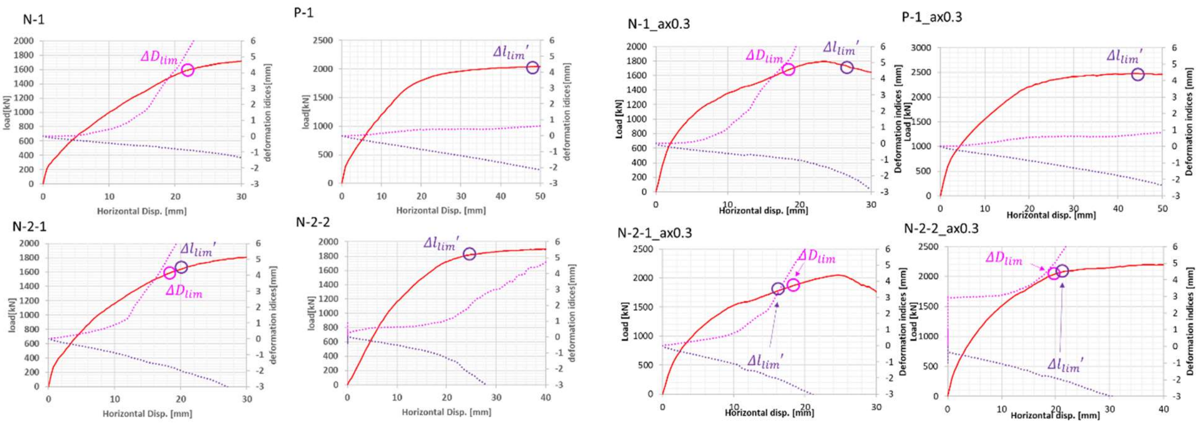

Figure 8. Load-displacement relationships and deformation indices in the case of axial force ratios of 0 or 0.3.

For N-2-1, when the axial force ratio was zero, the failure mode was oblique tensile failure. However, for N-2-1_ax0.3, the maximum principal strain contour diagram (deformation at 10 times magnification) in Figure 9 indicates that the diagonal crack toward the base of the column resulted in concrete spalling due to the substantial action of the axial force. The order of the indices is considered to have been reversed because the axial force acted on the column and the failure mode became shear-compression failure.

Regarding N-2-2, when the axial force was zero, the failure was compressive shear failure. However, for N-2-2_ax0.3, the maximum principal strain contour diagram (Figure 9, shown at the end of step 4) reveals that the growth of diagonal cracks was promoted by the significant action of the axial force.

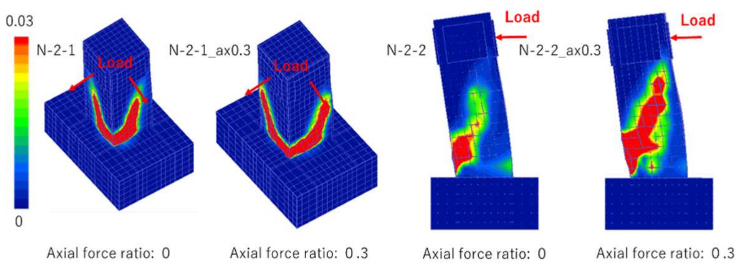

Figure 9. Maximum principal strain contour diagram with 10 times magnification of the deformation.

Thus, the deformation index accurately captures subtle changes in the failure mode. In addition, one of the indices reached its limit value while retaining about 90% or more of the maximum carrying capacity.

Verification of the Influence of Column Shape (Aspect Ratio 7.0 or 0.7)

Here, two analysis models with respective member thicknesses of 440 mm and 4,400 mm (approximately the upper and lower limits of the actual structure) are discussed assuming that the height of the columns remains the same. From a durability perspective, the cover of the main reinforcing bar was 100 mm regardless of the member thickness, and the cover depth was thus kept constant. Therefore, the aspect ratio (column height/thickness) was 7.0 for the model with member thickness of440 mm and 0.7 for the model with member thickness of 4,400 mm. The identifier of each analysis case indicates the value of the aspect ratio after the loading pattern (e.g., "N-1_as7.0").

Regarding the limit value of "Thickness increment of RC member," when the aspect ratio is 7.0, ΔD_{lim} = 5 mm in all cases. However, when the aspect ratio is 0.7, Eq. (2) applies, resulting in ΔD_{lim} = 8.8 mm for N-1, P-1, N-2-2, and ΔD_{lim} = 12.4 mm for N-2-1.

Figure 10 shows the load-displacement relationship when the aspect ratio is 7.0 or 0.7, with the points where both indices reach the limit values indicated by symbol "○". The investigation of verification indices when the aspect ratio is 2.8 are depicted in the left side of Figure 8. In analysis cases N-1_as7.0, N-1_as0.7, N-2-1_as7.0, and N-2-1_as0.7, the results were different from those in cases N-1 and N-2-1.

For analysis case N-1_as7.0, the stiffness and maximum load carrying capacity are smaller than those of other cases such as N-2-1_as0.7. Because the cover thickness is 100 mm for a member thickness of 440 mm, the stirrup is placed on the tensile side with respect to the position where the resultant force of the compressive stress acts. Therefore, the number of stirrups across the diagonal cracks is considered to have decreased, and the resistance to shearing force exerted is considered to be insufficient.

When the load acts in the diagonal direction (N-2-1_as0.7), the index that reaches the limit value differs from that in the analysis case N-2-1_as7.0 of the same loading pattern. In addition, the limit value was reached at a value slightly smaller than the maximum load capacity, likely because the thickness of the member and the damage to the base of the corner both increased. However, in each analysis case, the deformation index reached the limit value before or near the maximum load capacity. and the index reaches its limit value while retaining approximately 70% or more of its maximum load carrying capacity.

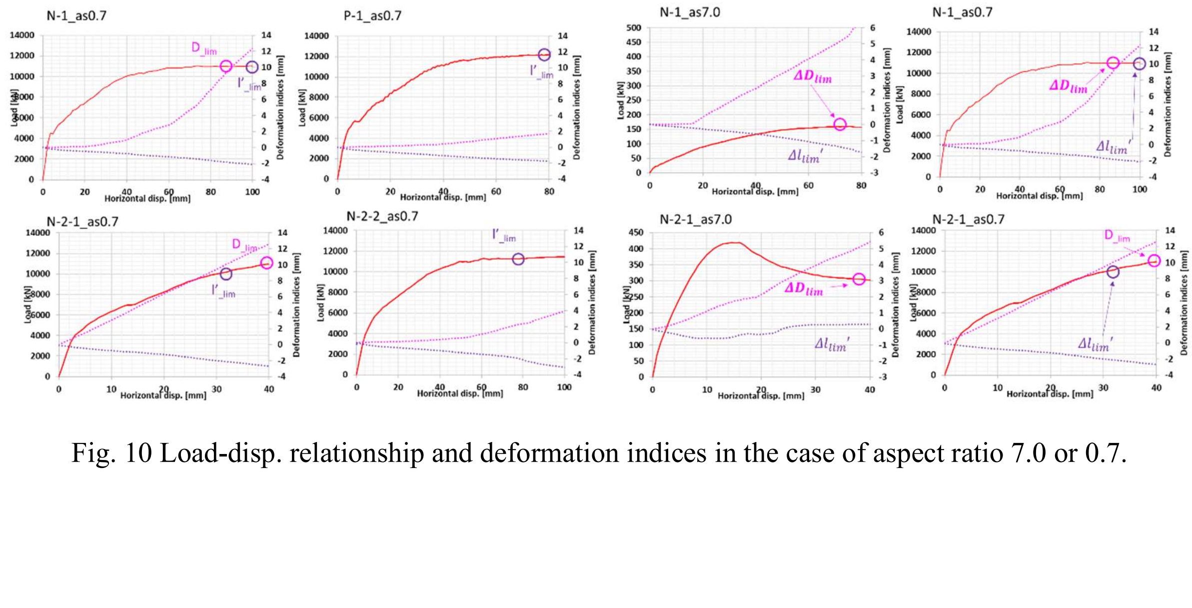

Fig. 10 Load-disp. relationship and deformation indices in the case of aspect ratio 7.0 or 0.7.

CONCLUSIONS

In this study, the authors analytically examined novel seismic performance verification indices under conditions simulating the service environment of the structures to be verified in order to increase and confirm the limits of applicability. As a result, the following conclusions were obtained:

(1) Within the scope of this study (axial force ratio of 0.3 or less), the limit value was reached with one of the proposed indices while sustaining a load of approximately 90% or more of the maximum load capacity. This finding suggests that the failure mode can be reliably estimated.

(2) Within the scope of this study (aspect ratio from 7.0 to 0.7), one of the proposed indices reached the limit value while maintaining a load of approximately 70% or more of the maximum load capacity. It was also revealed that the failure mode could be estimated. In the case of analysis with large aspect ratios, one of the deformation indices reached the limit value after the maximum load carrying capacity was reached. On the other hand, in the analysis case where the load was applied in the direction of the column corner with a small aspect ratio, the load-carrying performance was evaluated somewhat conservatively.

Considering the above results (for axial force ratio and specimen dimensions), the conditions applicable to these indices include an average axial force ratio of members of 0.3 or less and a minimum member dimension of 0.4 m.

ACKNOWLEDGEMENTS

We thank Professor Maekawa at Yokohama National University for his valuable guidance in conducting the analytical studies.

REFERENCES

JSCE (2018). *Standard Specifications for Concrete Structures - Design,* Japan Society of Civil Engineers, Tokyo. (in Japanese)

Komatsu, S., Miyagawa, Y. and Matsuo, T. (2021). "A Study on Application of Strain Indices for Seismic Performance Verification to Real-Scale RC Member by 3D Material Nonlinear FEA," *Proceedings for the 2021 fib Symposium*, Portugal.

Komatsu, S., Miyagawa, Y., Matsuo, T., Hata, A., Shimabata, T. and Nakamura, H. (2023). "Applicability of Deformation Indices Reasonably Evaluating Load Carrying Capacity and Failure Mode of Full-Scale RC Members Subjected to Bilateral Loads," *Journal of Advanced Concrete Technology,* 21(5), 421-435.

Maekawa, K., Pimanmas, A. and Okamura, H. (2003). "Nonlinear Mechanics of Reinforced Concrete," *Taylor & Francis Group*, Spon Press.

Miyagawa, Y., Nagata, S. and Matsumura, T. (2014). "Lateral Expansion and Residual Load Capacity of Reinforced Concrete Members Without Transverse Reinforcement," *Journal of Japan Society of Civil Engineers, Ser. E2 (Materials and Concrete Structures)*, 70(4), 402-416. (in Japanese)

Miyagawa, Y., Shibayama, A., Morozumi, H. and Shigemitsu, N. (2018). "Entire Displacement Distribution of Reinforced Concrete Box Culvert in the Damaging Progress Subjected to Horizontal Load," *Proceedings for the 2018 fib Congress*, Melbourne, 626-645.

Nuclear Power Civil Engineering Committee (2021). *Expansion Version of Guideline and Recommendation for Seismic Performance Verification of Critical Underground Reinforced Concrete Structures in Nuclear Power Plants,* Nuclear Power Civil Engineering Committee, Japan Society of Civil Engineers, Tokyo. (in Japanese)